AAV Application Notebook

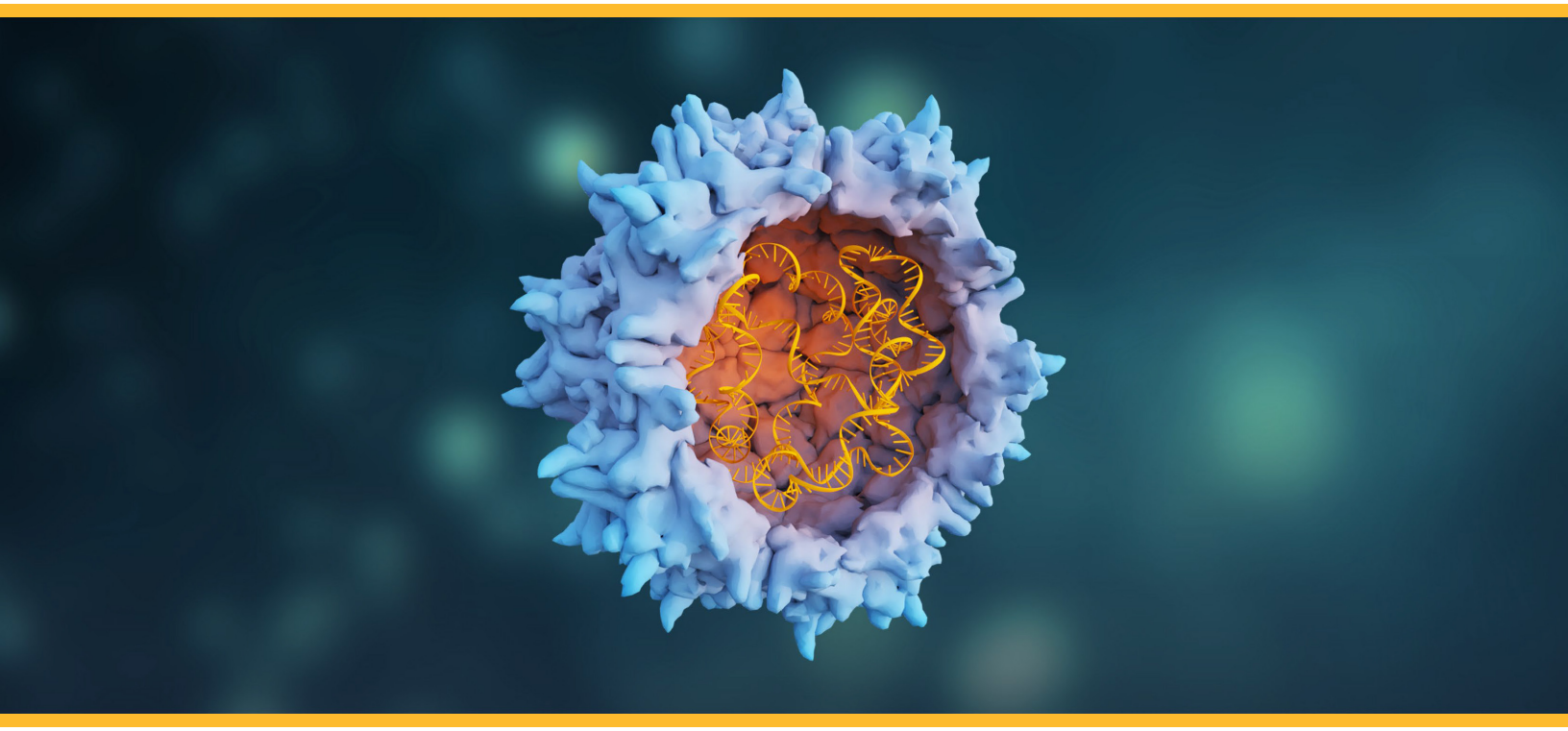

1. Quantifying quality attributes of AAV gene therapy vectors by SEC-UV-MALS-dRI
2. Why and how to quantify AAV aggregates by FFF-MALS
3. Characterization of AAV-based viral vectors by DynaPro DLS/SLS instruments

Wyatt Technology provides essential instrumentation and methods for quantifying critical quality attributes of AAV-based therapeutics. To learn more about these and other services for method implementation, training and SOP guidance, visit the AAV Services page.

WYATT TECHNOLOGY

APPLICATION NOTE

AN1617: Quantifying quality attributes of AAV gene therapy vectors by SEC-UV-MALS-dRI

Michelle Chen, Ph.D. and Anatolii Purchel, Ph.D., Wyatt Technology Corporation

Summary

The adeno-associated virus (AAV) is an attractive delivery vehicle in gene therapy[1,2] attributed to its mild immune response and ability to deliver its genetic payload into a wide range of host cells. The first FDA-approved AAV-based gene therapies are Luxturna® by Spark Therapeutics and Zolgensma® by Novartis for treating a rare genetic eye disease and spinal muscular dystrophy, respectively. With these approvals and many other AAV-mediated *in vivo* gene therapy drug candidates in clinical trials, it is essential that robust and reliable characterization tools are implemented in order to understand the quality attributes of this class of therapeutic products, ensuring their safety and efficacy[3].

A size-exclusion chromatography (SEC) method using triple detection–UV, differential refractive index (dRI), and multi-angle light scattering (MALS)–has been developed to measure the following three important AAV quality attributes (QAs): 1) Total number of viral capsid particles; 2) Relative capsid content (e.g., ratio of empty and full capsids); and 3) Percentage of monomer or aggregates.

Introduction

AAVs are small, single strand DNA viruses from a family of *Parvoviridae* that have become a popular viral vector for gene therapy due to their ability to infect both dividing and quiescent cells, their ability to persist in an extra-chromosomal state, and their absence of pathogenicity to the host target. Because of the stringent requirements imposed by health authorities, the AAV products throughout the manufacturing process need to be exceptionally well characterized. Some of the critical quality attributes (CQAs) of the AAV products include physical viral titer, capsid content, and product stability[4].

The measurement of the aforementioned QAs—especially the viral titer and the vector genome concentration—commonly involves approaches such as ELISA, qPCR, TEM, cryo-EM, analytical ultracentrifugation (AUC), or optical density measurements [5,6]. All these techniques are time-consuming, labor-intensive, and costly; some suffer from data inconsistency and lack of linearity for quantitation. As a result, it is difficult to implement them during the production process of the viral vectors.

In this application note, we present a simple, robust, and direct SEC method with UV-MALS-dRI detection. This method allows rapid sample analysis—with a total run time under 30 minutes per sample. The method can be readily employed to quantify AAV particle concentration, capsid content, and aggregation throughout the AAV product development and manufacturing processes.

Materials and Methods

AAV9 samples were received from Virovek Inc. (https://www.virovek.com/), which specializes in large-scale AAV production. Two samples were used for this application note: an empty AAV (no DNA payload) denoted as 'Empty' and a full AAV (a single-stranded DNA of full-length payload) as 'Full'. Empty and Full AAV samples were mixed at five different ratios (v/v), 1:1, 1:2, 1:3, 1:5, 1:10, for the analysis of relative capsid content. All samples were screened with a DynaPro® Plate Reader for the presence of large aggregates before injecting onto the HPLC system.

An Agilent 1260 Infinity II HPLC system was employed with a Wyatt WTC-050S5 column (7.8 x 300 mm) and the corresponding guard column. Phosphate-buffered saline was used as the mobile phase at a flow rate of 0.5 mL/min. The volume of each injection was 30 µL.

The detection system consisted of the Agilent HPLC's UV-Vis detector measuring at wavelengths of 260 nm and 280 nm, a DAWN® MALS detector with a WyattQELS® embedded online dynamic light scattering (DLS) module, and an Optilab® dRI detector. Data from the MALS, DLS,

UV (both wavelengths), and dRI detectors were collected and processed using ASTRA® software.

Results and Discussion

The dRI chromatograms obtained from two injections of the Empty and Full AAV samples are shown in Figure 1. ASTRA data analysis revealed that the aggregates and fragments were well separated from the main monomer peak without observable peak tailing. Excellent reproducibility in retention time and peak area were obtained from duplicate injections, and the peak area is linearly correlated with injection amount. These observations suggest that the SEC method developed for these two AAV samples is optimized and full mass recovery from the SEC column is likely achieved.

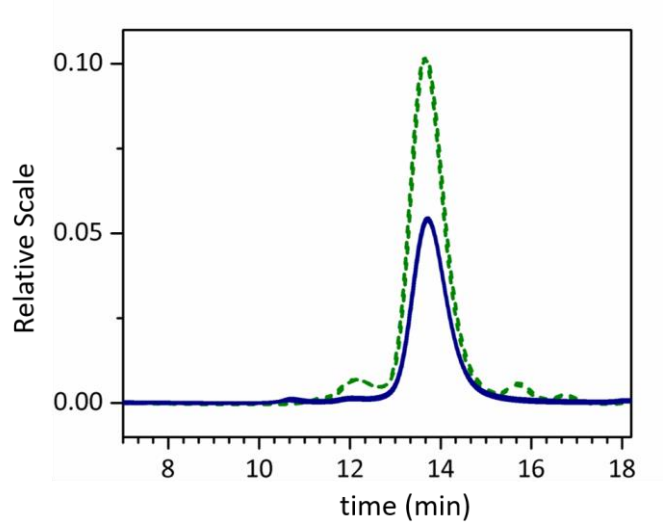

Figure 1. The dRI chromatograms obtained from two injections of Empty (green dashed line) and Full (blue solid line) samples are overlaid.

The UV extinction coefficients of the protein capsid and DNA payload were determined using the dRI and UV signals measured for the Empty and Full AAV samples along with the known d*n*/d*c* values of the capsid's protein shell (0.185 mL/g) and encapsulated DNA (0.170 mL/g). The extinction coefficients at 260 nm were found to be 1.3 mL/(mg·cm) and 25 mL/(mg·cm) for the protein and DNA, respectively. The extinction coefficients at 280 nm are 2.1 mL/(mg·cm) and 15 mL/(mg·cm) for proteins and DNA, respectively. It should be noted that for different serotypes and mutated capsid proteins, the extinction coefficients of the corresponding capsid may vary slightly.

Many important biophysical parameters of the AAV samples are obtained from ASTRA's *Protein Conjugate Analysis* features. These parameters include molar masses of the capsid and DNA, as well as the root mean square radius (a.k.a. radius of gyration) R_g and hydrodynamic radius R_h, all summarized in Table 1. The molar mass results for the Full AAV samples with respect to elution time are plotted in Figure 2, which illustrate the total molar mass of the Full AAV as well as the molar masses for the protein capsid and the encapsulated full-length DNA molecule.

Table 1. Molar mass and radius results for Empty and Full AAVs.

Sample/ injection	M_{capsid} [MDa]	M_{DNA} [MDa]	R_g [nm]	R_h [nm]
Empty/1	3.76±0.01	0	10.6±0.1	13.3±0.4
Empty/2	3.77±0.01	0	10.6±0.1	13.3±0.4
Full/1	3.77±0.01	1.16±0.01	9.8±0.1	13.4±0.3
Full/2	3.77±0.01	1.16±0.01	9.8±0.1	13.3±0.3

The eluted mass of both the protein capsid and DNA can also be measured by the *Protein Conjugate Analysis*. When combined with molar mass, either measured or theoretical, the mass can be converted to the three important quality attributes of an AAV sample: total particle concentration, relative capsid content, and percentage of aggregation.

Total particle concentration

The total AAV particle concentration, also referred to as particle titer or capsid concentration, is calculated using Equation (1):

$$C_{AAV} = m_P \times N_A / (M_{Capsid} \times v) \quad (1)$$

where C_{AAV} is the total AAV particle concentration, m_P is the total eluted protein mass, N_A is Avogadro's number, M_{Capsid} is the viral capsid's molar mass, and v is the injected volume of the AAV sample. For the Empty and Full samples used in this study, the total particle concentrations are 8.9×10^{13} mL^{-1} and 4.0×10^{13} mL^{-1}, respectively.

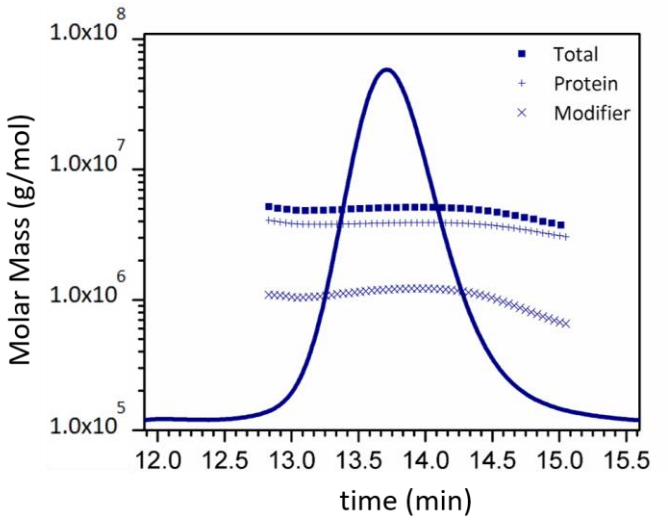

Figure 2. Molar masses for the Full AAV sample (■), protein (+), and DNA (x) are shown here overlaid with the dRI chromatogram.

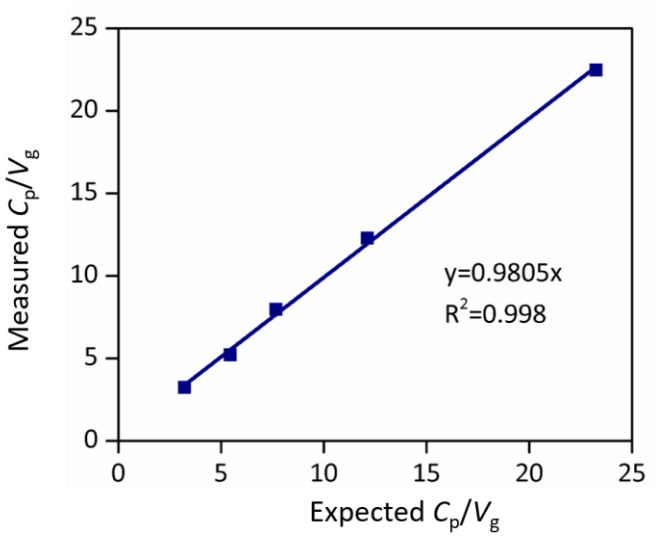

Figure 3. Plot of measured C_p/V_g from five mixtures of the Empty and Full samples at different ratios against the expected C_p/V_g values.

Capsid content

An AAV sample during production often contains both empty *and* full AAV particles. It is critical to reliably determine the percentages of empty and full AAV particles, i.e., the capsid content in the sample, in order to meet the production and purification goals as well as the final specification of an AAV product. The total AAV concentration can be calculated using Equation (1). The concentration of full AAV particles in the AAV sample, C_{full}, can be calculated in a similar way, shown in Equation (2), by using the total eluted DNA mass, m_{DNA}, and the molar mass of the full-length DNA molecule, M_{Full}.

$$C_{full} = m_{DNA} \times N_A / (M_{Full} \times v) \quad (2)$$

Once the concentrations of the total capsids and full AAV particles are known, the concentration of the empty capsids, C_{empty}, is simply their difference.

$$C_{empty} = C_{AAV} - C_{full} \quad (3)$$

Multiple terms derived from C_{AAV}, C_{full}, and C_{empty} can be used to express the AAV capsid content. These terms include Empty AAV%, Full AAV%, Full/Empty, Empty/Full, C_p/V_g or V_g/C_p, where C_p stands for capsid particle titer and V_g is viral genome titer.

A validation test on C_p/V_g was carried out by testing five mixtures of the Empty and Full AAV samples at different ratios as shown in Figure 3. Excellent agreement between measured and expected values was obtained as seen from the plot.

AAV aggregation

Using the equations from the previous sections, we calculated capsid concentrations of the monomer peak and the entire AAV peak to obtain the monomer percentage and aggregate percentage for both the Empty and Full AAV samples. The monomer in the Empty and Full sample is approximately 92% and 99%, respectively.

Large aggregates can be altered or removed by the SEC column separation mechanism. For AAV samples containing large aggregates, field-flow fractionation (FFF) employing an Eclipse™ system is used as an alternative or orthogonal tool for separating and quantifying aggregation, since FFF has no stationary phase that can interact with or damage the AAV samples.

These quality attributes were also measured on different SEC-MALS setups and by two different analysts. The results show that the method is highly robust and consistent when the SEC conditions are optimized.

Conclusions

The SEC-UV-MALS-dRI method measured particle concentration, relative capsid content, aggregation, and other quality attributes of AAV-based gene therapy vectors reproducibly and consistently. No a priori knowledge about the AAV structure or content is required. Similar methods incorporating these instruments have been validated and used in regulatory filings, manufacturing, and quality control for other biologics. As a result, we believe this method can be implemented in the AAV manufacturing

process and serve as a release assay for different production lots.

Acknowledgments

We thank Virovek Inc. for kindly supplying the AAV samples used in this study.

References

1. Bak, R. O. & Porteus, M. H. CRISPR-Mediated Integration of Large Gene Cassettes Using AAV Donor Vectors. *Cell Rep.* **20**, 750–756 (2017).
2. Hastie, Eric, and R. Jude Samulski. "Adeno-associated virus at 50: a golden anniversary of discovery, research, and gene therapy success—a personal perspective." Human gene therapy 26, no. 5 (2015): 257-265.
3. Gavin, D. K. FDA statement regarding the use of adeno-associated virus reference standard materials. *Hum. Gene Ther. Methods* **26**, 3 (2015).
4. Naso, Michael F., Brian Tomkowicz, William L. Perry, and William R. Strohl. "Adeno-associated virus (AAV) as a vector for gene therapy." BioDrugs 31, no. 4 (2017): 317-334.
5. Wright, J. F. "Manufacturing and characterizing AAV-based vectors for use in clinical studies." Gene therapy 15, no. 11 (2008): 840.
6. Smith, Peter H., Sumathy Parthasarathy, Jesse Isaacs, Sharmila Vijay, Jane Kieran, Sharon K. Powell, Alan McClelland, and J. Fraser Wright. "Quantification of adeno-associated virus particles and empty capsids by optical density measurement." Molecular Therapy 7, no. 1 (2003): 122-128.

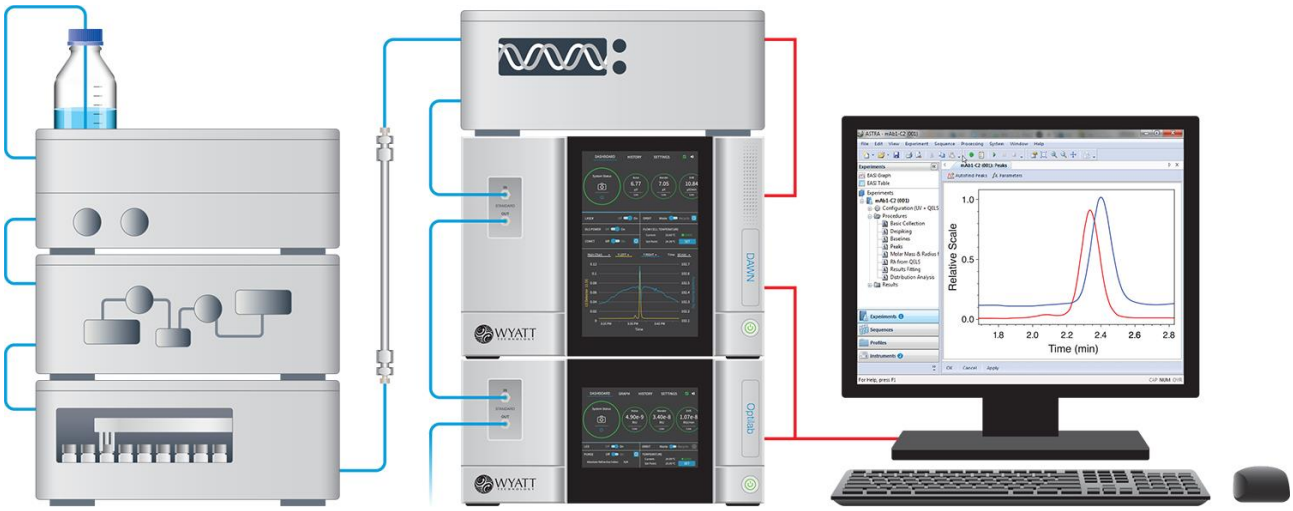

APPLICATION NOTE

AN2004: Why and how to quantify AAV aggregates by FFF-MALS

Judit Bartalis, Ph.D., Novartis Gene Therapies
Michelle Chen, Ph.D. and Daniel Some, Ph.D., Wyatt Technology Corporation

Summary

The percentage of aggregate is a critical quality attribute (CQA) of DNA-based therapeutics delivered by the engineered adeno-associated virus (AAV). This application note compares two platforms for analytical separations—size exclusion chromatography (SEC) and field-flow fractionation (FFF)—along with three online detection methods—UV, fluorescence, and multi-angle light scattering (MALS). The results demonstrate that FFF-MALS is the most appropriate method for quantifying all aggregates of AAV-mediated products, from dimer, trimer, and small oligomers to large aggregates.

Introduction

Owing to its recent medical successes, AAV has emerged as the most popular gene vector for delivering small gene therapeutics[1]. Ensuring the safety and efficacy of an AAV-encapsidated DNA product requires the identification and quantification of its CQAs, which must be monitored throughout the development and production cycle[2].

AAV aggregation depends on many factors including serotype, capsid titer, empty/full ratio, formulation buffer composition, storage, and stress conditions. Aggregates in an AAV product—just as in protein-based therapeutics—may decrease efficacy and increase immunogenicity, which may lead to immune-related adverse effects. Hence the degree of aggregation is one of the CQAs that must be monitored throughout the AAV product lifecycle.[3,4].

Size exclusion chromatography with ultra-violet absorption detection (SEC-UV) has been widely used to quantify the aggregation in therapeutic proteins and has been considered for AAV-based gene therapy products as well. For AAVs, the addition of a fluorescence detector (FLD) to the SEC-UV system will enhance detection sensitivity due to intrinsic fluorescence of the analyte. A MALS detector is often added as well, to help understand the aggregation profile and measure other AAV CQAs[5-8].

FFF is a size-based separation technique, orthogonal to SEC, that does not incorporate a stationary phase or an affinity-dependent mechanism of action. Combined FFF and SEC data constitutes comprehensive evidence to convince regulatory authorities that all aggregates are detected and quantified in the therapeutic product[4,8].

We discuss the strengths and limitations of these separation and detection tools for aggregate quantification and reveal some specific details for correctly quantifying AAV aggregates by MALS.

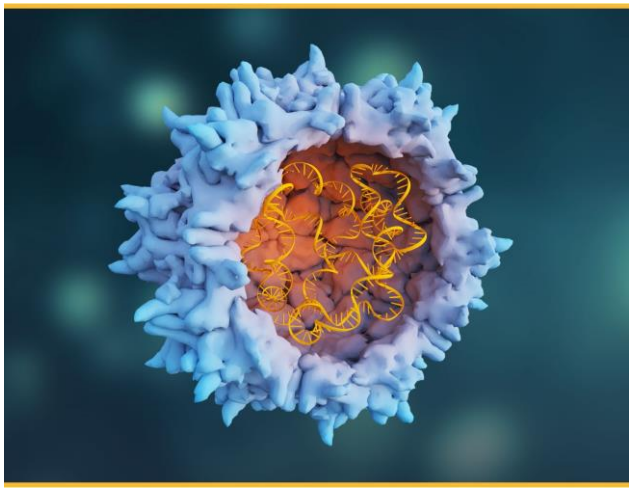

Materials and Methods

AAV samples were produced in-house at Novartis Gene Therapies and consist of four preparations with descending level of aggregation. The key sample properties are summarized in Table 1.

These preparations were pre-screened by DLS using a DynaPro® Plate Reader with DYNAMICS® software, to assess size and size distribution, and to confirm measurable differences in aggregation.

Table 1. Details of the AAV samples used in this note.

Sample ID	Type of Capsid	Aggregation level
Sample A	Empty	Level 4
Sample B	Empty	Level 3
Sample C	Empty	Level 2
Sample D	Full	Level 1

SEC-MALS-UV-FLD instrumentation

An Acquity UPLC system from Waters Corp., equipped with FLD and PDA UV detectors, was employed for SEC separation and quantification. For some measurements, a DAWN® MALS detector was also added for molecular weight (MW) and size analysis. An appropriate SEC column was used to resolve AAV monomer and its oligomers with phosphate buffer saline as the mobile phase. Data from UV absorbance at 280 nm and fluorescence with 280 nm excitation/350 nm emission were collected with Empower software. ASTRA® software was used to collect and analyze MALS data.

FFF-MALS-UV-FLD instrumentation

FFF separation was carried out with an Eclipse™ FFF instrument and separation channel supported by an Agilent 1260 Infinity II HPLC pump and autosampler. Online detectors included a DAWN MALS instrument, an Optilab® dRI detector, and Agilent 1260 Infinity II FLD and MWD UV detectors. The FFF system was controlled by OpenLab with the Eclipse plug-in, while data were collected and processed by ASTRA. Separation took place in an Eclipse short channel with a 350 µm spacer and regenerated cellulose (RC) membrane (10 kDa cutoff). Phosphate-buffered saline (PBS) was used as the running buffer at a detector flow of 0.6 mL/min.

An optimal FFF separation method was developed. For analysis, at least two injections were made for each sample to assess the reproducibility of the method. The injection amounts were approximately $6x10^{11}$ AAV particles for all SEC and FFF runs. AAV particle concentration and the total volume of particles contained in each peak were calculated from MALS data with ASTRA's *Number Density* method. The sphere model was used with correction factors applied to account for the non-spherical shape of the different aggregates[9].

Results and Discussion

Though an AAV, with an approximate radius of 13 nm, is much larger than most proteins, SEC with a large pore size column (e.g., 450 to 2000 Å) is still appropriate for separating AAV monomer, small aggregates, and fragments. However, as we have learned from working with protein therapeutics, large aggregates can be dissociated by column shear, dilution, or solvent exchange, or directly removed by the column acting as a filter[10,11]. Because of this limitation of SEC, FFF is required to assess aggregation of AAV products, even more so than for protein therapeutics.

SEC removes large AAV aggregates

All four AAV samples were analyzed by SEC and FFF with UV and FLD detectors. The UV and FLD traces from both SEC and FFF of Sample A (the sample containing the most aggregates) are shown in Figure 1. Note that the elution order in FFF is reversed relative to SEC: larger particles elute earlier in SEC but later in FFF. The peak corresponding to large aggregates was only observed in FFF (39 to 46 minutes) and not in SEC (before 10.5 minutes). These results imply that SEC—even using a column packed with large pore sized beads—cannot preserve and properly elute the large aggregates.

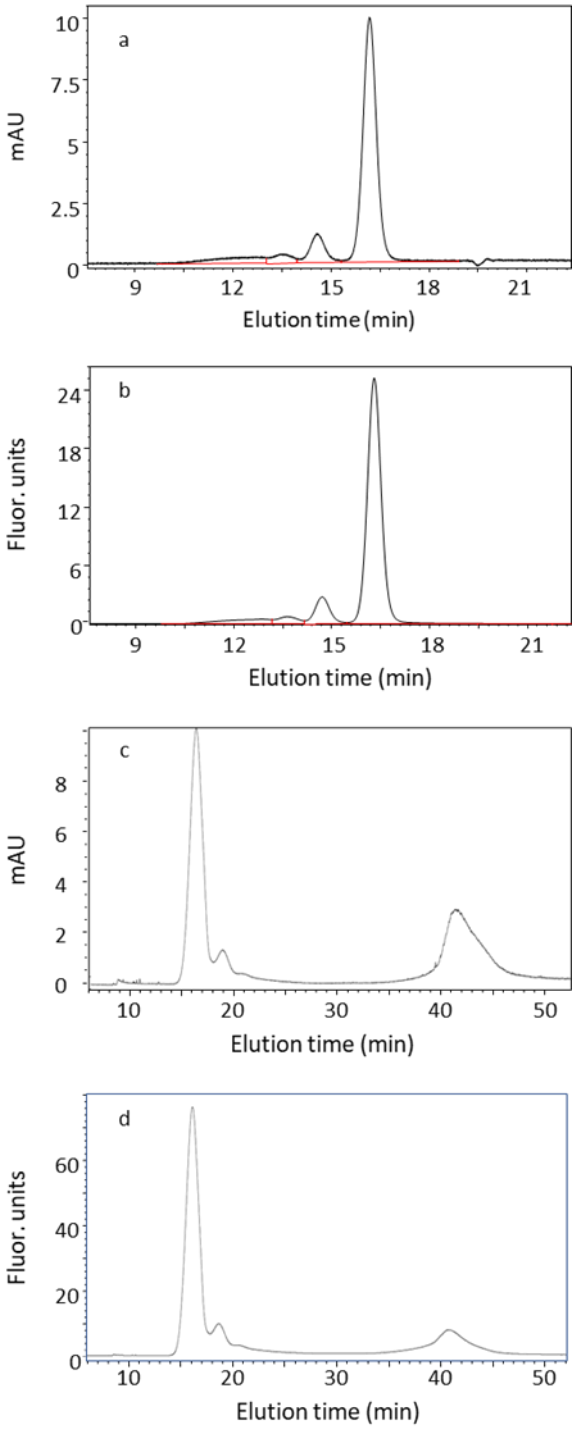

Figure 1. SEC-UV (a) and SEC-FLD (b) chromatograms and FFF-UV (c) and FFF-FLD (d) fractograms of AAV Sample A.

We compare the MALS data obtained from SEC and FFF for Samples A, B and C in Figure 2, where the radius determined by MALS is overlaid with the LS fractogram, plotted against elution time. The radius plotted here is the geometric radius, calculated by fitting angular data to ASTRA's sphere model. Under the conditions used for these measurements, SEC provided better resolution than FFF between monomer and dimer.

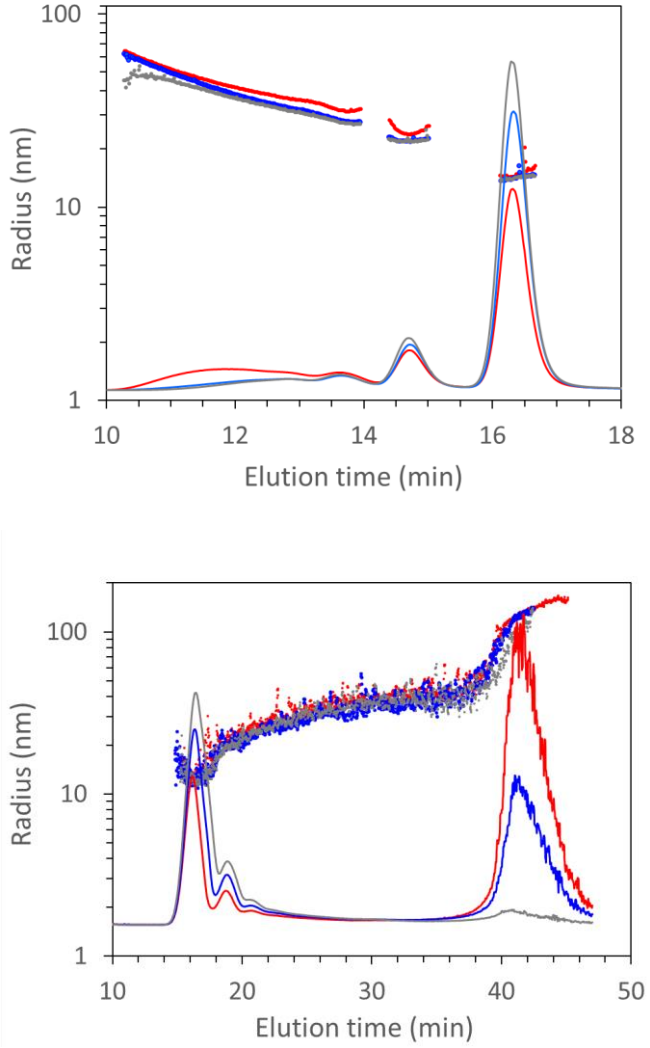

Figure 2. Radius versus elution time, overlaid with LS traces obtained from SEC-MALS (top) and FFF-MALS (bottom), for Samples A (red), B (blue) and C (gray), with descending degree of aggregation. SEC provides baseline separation of monomer and dimer, whereas FFF does not.

At the same elution time, radii from different samples were different in SEC but similar in FFF. This indicates that eluted aggregates were not as well separated in SEC as in FFF. The apparent large radii of dimer and trimer from Sample A in SEC are due to the co-eluted larger aggregates, which are prominent from 10 to 13 minutes but are believed to bleed into the dimer and trimer peaks. In addition, aggregates with radii greater than 60 nm (which will be referred to as large aggregates, L.A., in this note) were only detected by FFF-MALS, consistent with the other reports that the large aggregates are

removed by the column packing or column frits and possibly degraded by shearing[8].

Quantification of small oligomers is similar across methods

We then set out to compare the quantity of monomer, dimer, trimer, and oligomers, excluding the large aggregates, as determined by the three different detectors following the SEC and FFF separations. The results are shown in Figure 3, which plots the mass percentage of different AAV oligomeric states obtained under different combinations of separation platform and detection mode. Quantitation of mass percentage by UV and FLD is based on peak area, whereas quantitation by MALS makes use of the total particle volume calculation (provided by ASTRA software), corrected to account for oligomeric shape. Details of the correction will be discussed in the next section. Note that mass percentage and volume percentage are nearly identical quantities (after shape correction). Average values from duplicate injections were found to have a typical relative standard deviation of less than 5%.

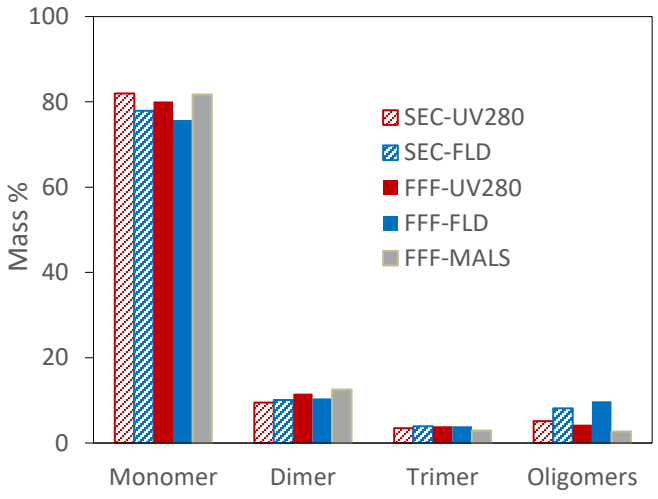

Figure 3. Quantitation of AAV oligomeric states in Sample A by SEC (stripped bars) and FFF (solid bars) using UV (red), FLD (blue), and MALS (gray) analyses.

Ignoring large aggregates, the mass percentages of monomer, dimer, and trimer from these five methods agree relatively well. For example, the measured monomer percentage varies across the methods from 74% to 82%, dimer percentage changes from 9% to 12% and trimer percentage from 3% to 4%. However, the mass percentage of oligomers differs noticeably: 3% from FFF-MALS, 4-5% by UV, and 8-10% by FLD. Note that the 'oligomer' peak includes tetramer, pentamer and larger aggregates, constrained to a radius of less than 60 nm. The average radius of the oligomers is about 36 nm, large enough to cause a scattering effect in UV and FLD signals which likely contributed the apparently higher mass percentage from these detectors, relative to the MALS result.[12]

The results in Figure 3 suggest that SEC-UV and SEC-FLD are adequate for quantifying the mass percentage of AAV monomer, dimer, and trimer. They are not appropriate, however, for quantifying larger AAV oligomers due to scattering artifacts. We will discuss similar observations with large aggregates in the next section.

UV and FLD overestimate large aggregates

The complete mass percentage results of all the AAV species–including the large aggregates–are tabulated in Table 2. As discussed above, this table reveals that the large aggregates were not detected when SEC served as the separation platform. Additionally, due to scattering of incident UV light in the respective detectors, quantitation by UV or FLD overestimates the mass percentage of large oligomers and especially of large aggregates.

Table 2. Mass percentage of AAV monomer (M), dimer (D), trimer (T), oligomer (O), and large aggregates (L.A.) of Sample A obtained from SEC and FFF with different detectors.

	M%	D%	T%	O%	L.A.%
SEC-UV	82.0	3.4	3.4	5.1	0.0
SEC-FLD	77.9	10.1	3.9	8.1	0.0
FFF-UV	48.6	7.0	2.1	1.9	40.4
FFF-FLD	61.4	9.1	3.0	6.4	20.1
FFF-MALS	86.8	6.4	1.4	2.2	3.2

To understand these results more fully, we plotted the mass fraction of each aggregate type normalized to monomer mass in Figure 4. It is evident that quantitation with UV and FLD overestimates the amount of aggregates larger than trimer, and greatly overestimates the L.A. fraction. These data and graphs enable us to conclude that FFF-MALS is the only method, among the five methods discussed in this note, that can properly separate and quantify **all** aggregates in an AAV sample.

FFF-MALS is the most appropriate method to quantify all AAV aggregates

As the most appropriate method for quantifying all AAV aggregates, FFF-MALS was then used to determine the mass percentage of each aggregate species in all four AAV samples listed in Table 1. The MALS fractograms from duplicate injections are shown in Figure 5.

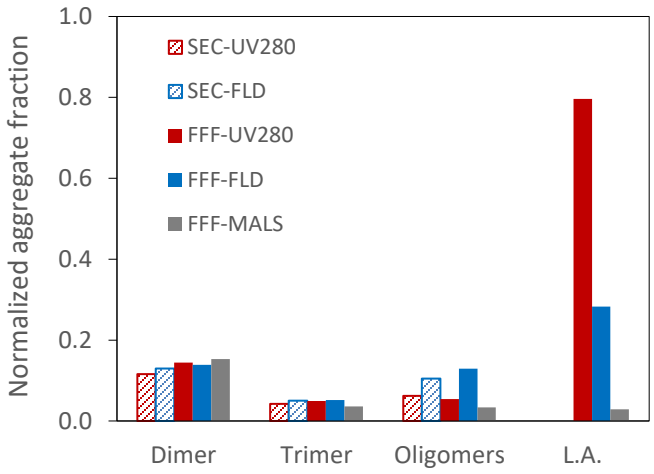

Figure 4. Aggregate fraction normalized to monomer mass in Sample A, separated by SEC' (stripped bars) or FFF (solid bars) and analyzed by UV (red), FLD (blue) or MALS (gray).

The perfectly overlapped traces from duplicate injections demonstrate the excellent reproducibility of the FFF-MALS method. The flat trace from a blank injection (injection of mobile phase), which were collected at the end of the data collection sequence, show negligible carryover under the FFF method employed.

Mass percentage is typically used to quantify aggregates. For UV and FLD, mass percentage is based on the areas of monomer and small oligomer peaks. UV and FLD detectors, however, cannot measure reliable mass percentage of large aggregates, as discussed in the previous section. MALS data and ASTRA software determine size, number of particles, and total volume of particles in each of the designated peak regions, enabling the peaks to be both unequivocally identified and quantified in terms of mass percentage.

For FFF-MALS, mass percentage is related to the total volume of particles in each peak, normally calculated under the assumption of uniform spheres with the same densities. However, AAV aggregates, especially small oligomers like dimer and trimer, deviate from a spherical model such that corrections must be applied. The correction factors for each type of aggregate are detailed in Table 3. We applied the shape correction factor to FFF-MALS data from all four AAV, with the results shown in Figure 6.

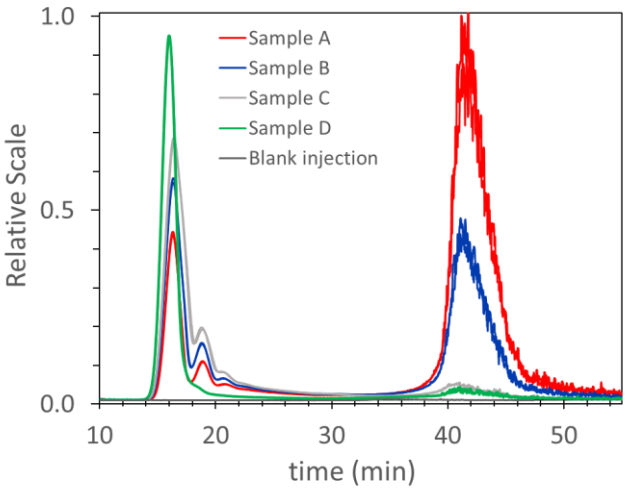

Figure 5. MALS fractograms of four AAV samples (red, blue, gray, and green traces), 2x each, and a 'blank' injection (black trace). Near-perfectly superimposed fractograms from duplicate injections demonstrate the reproducibility of the method.

Table 3. Correction factor of volume of particle for monomer, dimer, trimer, oligomers, and large aggregates (L.A.).

Aggregation state	Correction factor for volume
Monomer	1.00
Dimer	2.22
Trimer	1.96
Oligomer	1.39
L.A.	1.10

From Figure 6, we readily conclude that the concentration of large aggregates decreases in the order from Sample A to Sample D, consistent with the expected trend. For Sample D, the full capsid sample, there are no measurable large aggregates, and monomer accounts for 98.7% of the total injected mass. The aggregation trend found in the FFF-MALS results are consistent with the one observed from the DLS measurements (not shown).

Though FFF-MALS is the tool of choice for characterizing and quantifying all sizes of AAV aggregates, it may not always be required. When it has been demonstrated that large aggregate formation is not detected under typical

storage conditions, SEC-MALS is adequate for routine aggregate monitoring.

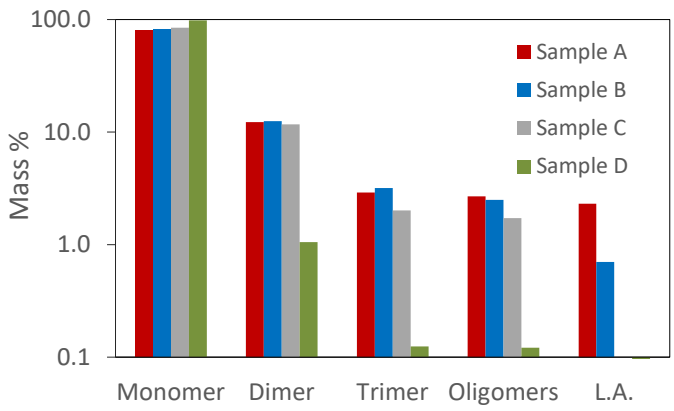

Figure 6. Mass percentage (logarithmic scale) of each aggregate type for the four AAV samples.

Conclusions

As more and more AAV-delivered gene therapy products come near to their final stages of clinical trials and begin commercialization, it is critical to accurately assess the amount of all aggregates in these products. Though SEC-UV and SEC-FLD are appropriate for measuring small aggregates such as dimer and trimer, they are inadequate for quantifying large oligomers and larger aggregates that may be present.

Large aggregates are shown to be susceptible to alteration and removal by the SEC column, making FFF the separation tool of choice for quantifying all the aggregates in an AAV sample. Furthermore, UV and FLD are not recommended for quantification by FFF. Due to scattering artifacts in these detectors, they overstate the quantity of larger aggregates. Applying the modified number density analysis to FFF-MALS data is the most appropriate method for measuring the mass percentage of aggregates, from dimer to large aggregates. With aggregates and other critical quality attributes accurately quantified and monitored, the safety and efficacy of AAV products can then be determined with greater certainty.

References

1. Bulcha, J. T. et al. (2021). Viral vector platforms within the gene therapy landscape. *Sig Transduct Target Ther* **6**, 53. https://doi.org/10.1038/s41392-021-00487-6
2. Gavin, D. K. (2015). FDA statement regarding the use of adeno-associated virus reference standard materials. Hum. *Gene Ther. Methods* **26**, 3. https://doi.org/10.1089/hgtb.2015.1501
3. Srivastava, A. et al. (2021). Manufacturing challenges and rational formulation development for AAV viral vectors. *Journal of Pharmaceutical Sciences*, **110**(7), 2609-2624. https://doi.org/10.1016/j.xphs.2021.03.024
4. Wright, J.F. et al. (2005). Identification of factors that contribute to recombinant AAV2 particle aggregation and methods to prevent its occurrence during vector purification and formulation. *Molecular Therapy* **12**(1), 171-178. https://doi.org/10.1016/j.ymthe.2005.02.021
5. McIntosh, N. L. et al. (2021). Comprehensive characterization and quantification of adeno associated vectors by size exclusion chromatography and multi angle light scattering. *Scientific Reports*, **11**(1), 1-12. https://doi.org/10.1038/s41598-021-82599-1
6. Chen, M. & Purchel, A. Wyatt Technology Application Note 1617: Quantifying quality attributes of AAV gene therapy vectors by SEC-UV-MALS-dRI. https://wyattfiles.s3-us-west-2.amazonaws.com/literature/app-notes/sec-mals-proteins/AN1617-AAV-CQA-Analysis-by-SEC-MALS.pdf
7. Kenrick, S., Purchel, A., & Chen, M. (2021). Quantifying AAV Quality Attributes Using SEC–MALS. *Column*, April 2021, Volume 17, Issue 04. https://www.chromatographyonline.com/view/quantifying-aav-quality-attributes-using-sec-mals
8. Deng, C. Wyatt Technology Application Note 2003: Quantifying AAV aggregation and quality attributes by FFF-MALS. https://wyattfiles.s3-us-west-2.amazonaws.com/literature/app-notes/fff-mals/AN2003-quantifying-AAV-aggregation-and-CQAs-by-FFF-MALS_CDeng.pdf
9. Wyatt, P. J. (2014). Measurement of special nanoparticle structures by light scattering. *Analytical chemistry*, **86**(15), 7171-7183. https://dx.doi.org/10.1021/ac500185w
10. Rosenberg, A. S. (2006). Effects of protein aggregates: an immunologic perspective. *The AAPS Journal*, **8**(3), E501-E507. https://dx.doi.org/ 10.1208/aapsj080359
11. Carpenter, J. F., Cherney, B., & Rosenberg, A. S. (2012). The critical need for robust assays for quantitation and characterization of aggregates of therapeutic proteins. In *Analysis of aggregates and particles in protein pharmaceuticals* (pp. 1-7). John Wiley & Sons, Inc., Hoboken, New Jersey.
12. Jia, X. et al. (2021) Enabling online determination of the size-dependent RNA content of lipid nanoparticle-based RNA formulations. *Journal of Chromatography B* **1186**, 123015. https://doi.org/10.1016/j.jchromb.2021.123015

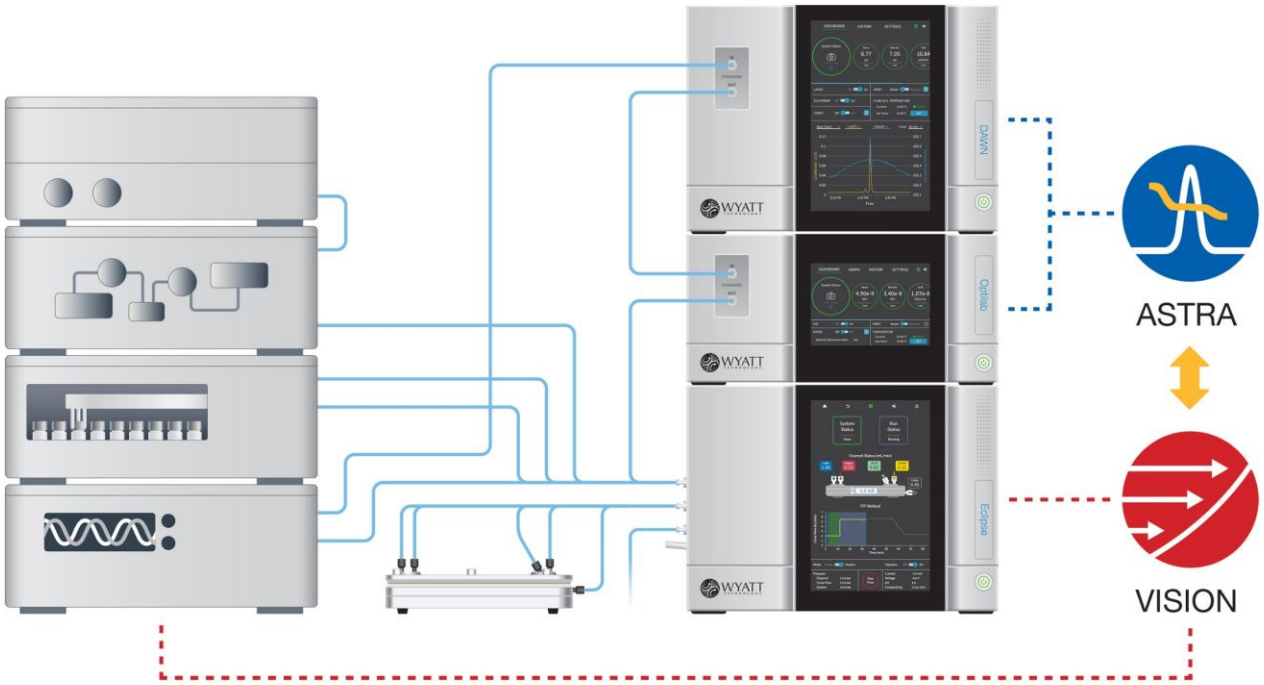

WYATT TECHNOLOGY

APPLICATION NOTE

AN5007: Characterization of AAV-based viral vectors by DynaPro DLS/SLS instruments

Xujun Zhang, Ph.D., Wade Wang, Ph.D., and Sophia Kenrick, Ph.D., Wyatt Technology Corporation

Summary

When developing adeno-associated virus vectors as drug products, multiple quality attributes must be monitored to ensure a safe and efficacious final product. Three such QAs are total AAV particle concentration, aggregate content, and thermal stability. The DynaPro® NanoStar® and DynaPro Plate Reader enable fast, easy measurements of these quality attributes in batch mode with combined dynamic and static light scattering.

Introduction

Adeno-associated virus (AAV) consists of a non-enveloped protein capsid with diameter ~25 nm, packed with single-stranded DNA. With a history of over fifty years of study, AAV has become one of the most popular and well-characterized gene-delivery vectors for clinical applications.[1,2]

To provide safe and effective gene-therapy products, several quality attributes (QAs) must be quantified throughout the development and manufacturing process. The most common quality attributes relate to stability, purity, and potency of the AAV product.[3]

A variety of analytical tools are used to monitor QAs of AAV vectors, including analytical ultracentrifugation (AUC) and real-time PCR. However, these techniques can be labor-intensive, costly, and destructive to the sample, making them unsuitable for early-stage, high-throughput screening. SEC-MALS is non-destructive, easier and faster than the aforementioned techniques. The use of SEC-MALS with a DAWN® multi-angle light scattering detector to characterize AAV QAs including size, aggregation, concentration and empty:full ratio is discussed in application note AN1617: AAV critical quality attribute analysis by SEC-MALS.

SEC-MALS provides detailed analysis, but requires 30 minutes per sample and may not be appropriate for screening of processes and formulations. In contrast, batch light-scattering techniques provide quick, easy, and high-throughput characterization of AAV solutions, albeit with limited resolution and accuracy in comparison. Here, batch static and dynamic light scattering (SLS and DLS) are used to quantify three AAV quality attributes:

1. Aggregate content
2. Thermal stability
3. Total viral particle concentration

This application note highlights all three measurements in both the DynaPro Plate Reader and DynaPro NanoStar DLS/SLS instruments.

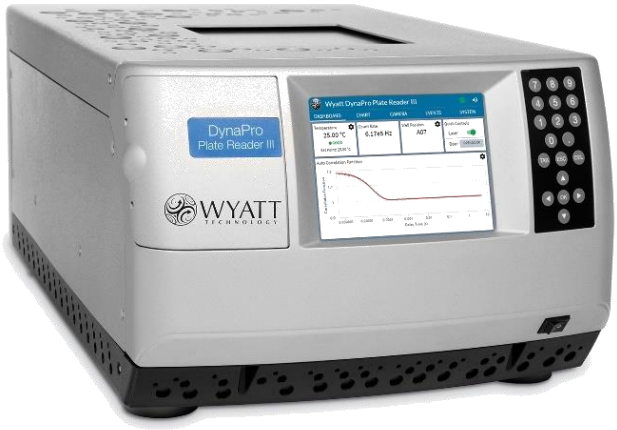

DynaPro Plate Reader performs dynamic and static light scattering measurements in standard 96, 384 or 1536 well plates.

Materials and Methods

AAV9 samples (Table 1) were kindly provided by Virovek, Inc. (https://www.virovek.com/), which specializes in large-scale AAV production. Samples S1 and S2 represented purified AAV samples that are either 'empty' (no DNA payload) or 'full' (containing full-length, single-stranded DNA). Sample S3 is an AAV with an unknown amount of DNA payload. Samples S4 through S7 represent investigations of various buffer conditions on the stability and aggregate content of the AAVs.

Batch DLS and SLS measurements were performed with the DynaPro NanoStar and DynaPro Plate Reader as described below. Data acquisition and analysis were performed with DYNAMICS® software.

Table 1: AAV sample description

Sample ID	AAV	Buffer	Note
S1	AAV9	A	Purified, empty
S2	AAV9	A	Purified, full
S3	AAV9	A	Unknown DNA payload
S4	AAV9	B	Formulation testing
S5	AAV9	C	Formulation testing
S6	AAV9	D	Formulation testing
S7	AAV9	E	Formulation testing

DynaPro NanoStar

Low-volume DLS and SLS measurements were performed with a DynaPro NanoStar to assess the size and size distribution for aggregation. For samples S1 through S3, 1.25 µL of neat AAV solutions were loaded into the quartz cuvette. Each measurement consisted of five 5-second acquisitions. DLS and SLS data were collected to determine hydrodynamic radius (R_h), aggregate content, molar mass, and viral particle concentration.

DynaPro Plate Reader

High-throughput measurements were made using the DynaPro Plate Reader. All measurements were performed in a 384-well microtiter plate (Aurora), and each well was loaded with 30 µL solution. The plate was centrifuged at 400 *g* for 1 minute prior to loading into the plate reader.

AAV samples S1 and S2 were diluted 1:10 in buffer. In addition, three mixtures of S1 and S2 were created with ratios of full:empty AAV corresponding to 1:1, 1:10, and 1:50 (v/v). Each AAV solution was loaded into the microtiter plate in triplicate, and each well was capped with 1-2 drops of silicone oil to prevent evaporation. DLS and SLS data were collected to determine R_h, aggregate content, and viral particle concentration at 25 °C. For thermal stability measurements, the temperature was ramped continuously from 25 °C to 85 °C at a rate of 0.1 °C/min, and R_h was measured throughout the temperature ramp.

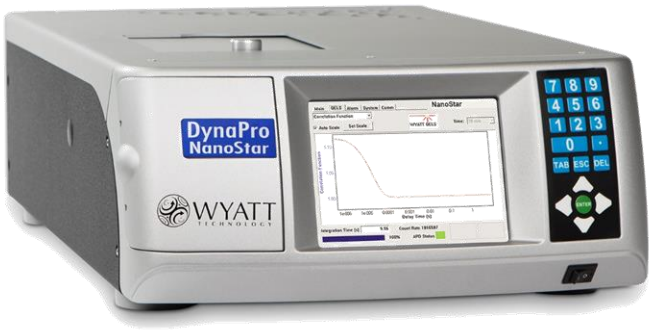

DynaPro NanoStar performs dynamic and static light scattering measurements in 1.25 µL quartz or 4 µL disposable cuvettes.

AAV samples S4 through S7 were loaded into single wells without dilution. The wells were sealed with tape (Nunc) to prevent evaporation. The plate was incubated at 37 °C for two hours, and the R_h distribution was measured over time to determine the effect of the formulation buffer.

Results and Discussion

Size and size distribution

Measuring the size and size distribution with batch DLS provides a quick approach to assessing the degree of aggregation in AAV solutions. Among the seven AAV samples tested, DLS revealed clear differences in particle size and aggregate content. Purified AAVs (S1 and S2), exhibited autocorrelation functions (ACF) with smooth, fast decays, characteristic of monodisperse samples of the expected size (Figure 1, top). In contrast, the autocorrelation functions for samples S4 through S7 decayed more slowly, indicative of larger aggregates present in the solution. Fitting the ACFs with a regularization algorithm provides the size distributions shown in the lower graph of Figure 1.

Purified AAV samples S1 and S2 appear to be uniform solutions with R_h = 14.7 ± 0.7 nm and 15.6 ± 0.1 nm, respectively. Furthermore, the weight-average molar mass (M_w)

determined by SLS with NanoStar are 3.67 ± 0.01 MDa for S1 and 6.78 ± 0.03 MDa for S2. The molar mass of S1 agrees well with the capsid molar mass measured by SEC-MALS.[4]

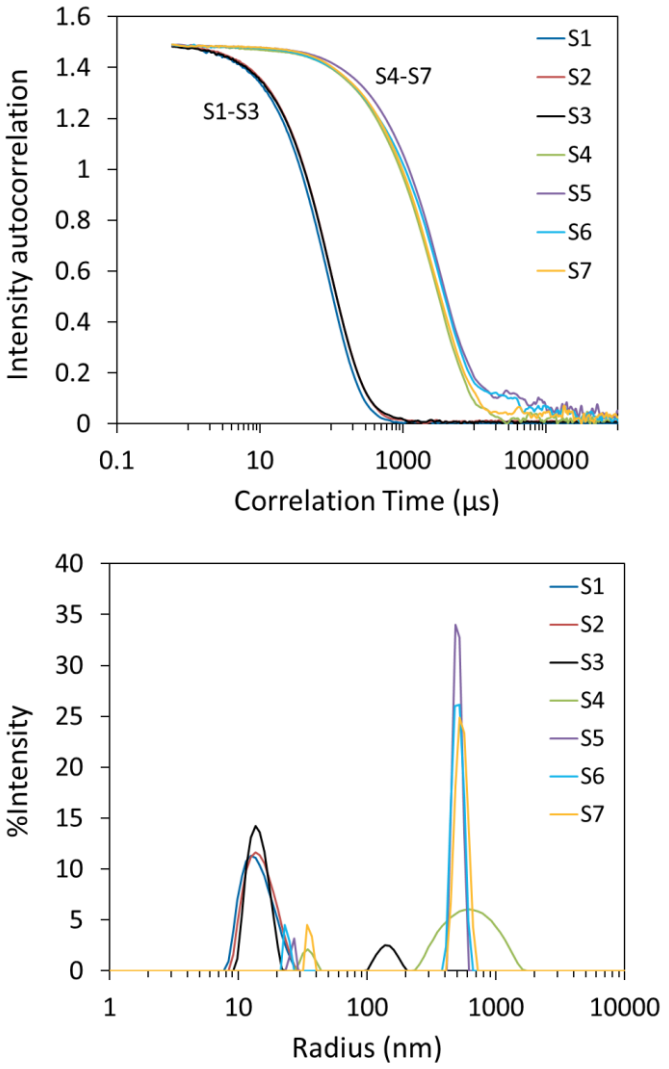

Figure 1. Autocorrelation functions (top) and size distribution via regularization (bottom) of AAVs for formulation screening.

The increase in molar mass in S2 is consistent with the incorporation of the DNA into the viral capsid; however, its apparent molar mass is slightly larger than the value of 4.93 ± 0.03 MDa determined by SEC-MALS.[4] This discrepancy in molar masses determined by (unfractionated) DLS/SLS and (fractionated) SEC-MALS is likely due to the nature of two methods. SEC-MALS separates aggregates from the monomer, and hence reports the molar mass of the monomer separately from oligomers. However, a batch DLS/SLS measurement reports the weight-averaged molar mass of the entire solution including monomer, dimer and higher-molecule-weight species.

Although the autocorrelation function for Sample S3 is only subtly different from samples S1 and S2 (Figure 1, top), the resulting distributions show that Sample S3 contains two size modes (Figure 1, bottom). The smaller mode, at ~ 15 nm, overlaps well with purified AAVs S1 and S2, and is consistent with monomeric AAV or a mixture of monomer and small quantities of oligomers. The second mode contains large aggregates with R_h ~100 nm.

Samples S4 through S7 appear to be highly aggregated (Figure 1). One size mode with average R_h ~ 30 nm corresponds to oligomers, and a second, with R_h ~ 550 nm, is due to large aggregates. The 30 nm mode appears quite small in terms of %Intensity but actually is dominant when viewed in the %Mass representation. These buffer conditions were thought to mitigate or promote different aggregate content. However, in this study those differences were not apparent at 25 °C, and were only noticeable upon incubation at 37 °C (see below).

Thermal stability

Two tests of thermal stability were performed in this study. First, the hydrodynamic radii of samples S1, S2, and their mixtures were measured throughout a continuous temperature ramp to quantify aggregation onset temperature T_{onset}. In addition, S4 through S7 were incubated at a constant temperature of 37 °C to observe changes in size and size distribution occurring at physiological temperature.

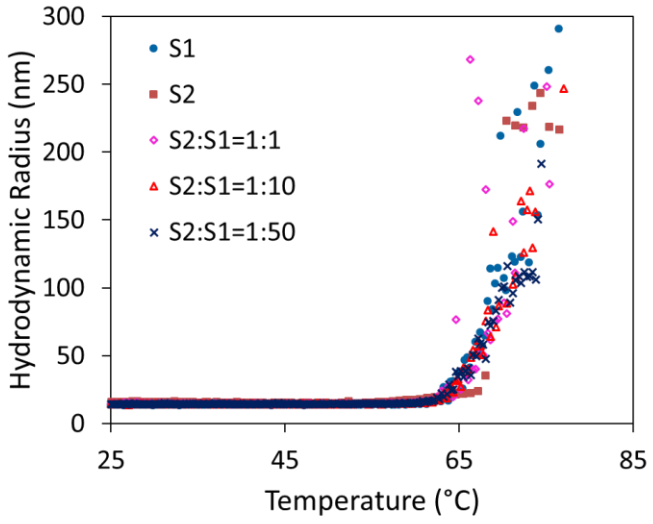

Figure 2. Aggregation screening of AAVs upon thermal ramping.

Both full and empty AAVs appeared to have the same T_{onset}, suggesting incorporation of the DNA payload does not change the thermal stability of the capsid. Figure 2 shows R_h as a function of temperature for empty AAV (S1), full AAV (S2), and three different mixtures. The size remains constant for all the samples until the temperature is increased beyond 60 °C. A sharp increase in R_h was then observed, growing from 14 nm to 300 nm, indicating the formation of aggregates. Onset analysis in DYNAMICS was used to determine T_{onset} and the corresponding radius for each sample. The onset temperature was the same across all samples at 62.5 ± 0.5 °C, and its corresponding onset R_h was 18.3 ± 1.1 nm.

The response of aggregated AAV samples (S4 through S7) to physiological thermal conditions was examined at a fixed incubation temperature of 37 °C. As shown in Figure 3, all four AAV solutions exhibit a decrease in R_h as a function of incubation time. At t = 0, the mean size of all four samples ranged from 450 nm to 530 nm, with S5 being the largest and S4 being the smallest. The rate of aggregate dissolution varied as a consequence of the different formulation additives, resulting in final mean sizes of 140 nm to 400 nm.

R_h decreased the most for S6, which was formulated with the highest concentration of a particular buffer ingredient. It was hypothesized that this component could prevent aggregation of AAVs, and may also enable recovery of monomers from aggregated samples.

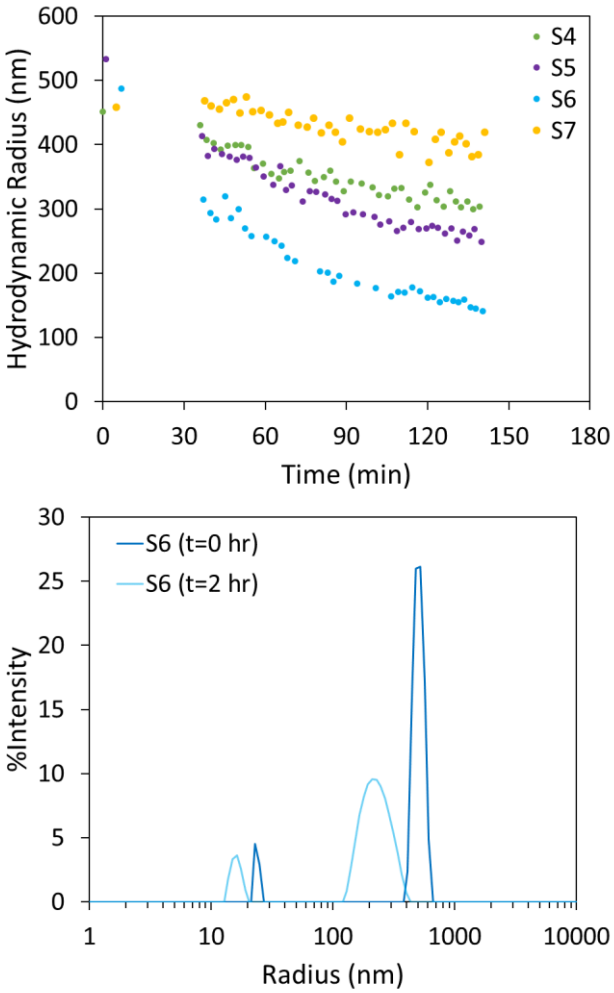

Figure 3. Top: R_h versus time upon incubation at 37 °C for AAVs in different formulations. Bottom: An example of evolving size distribution during incubation, sampled at t = 0 and t=2 hours.

Table 2. Size distribution and particle concentration by regularization in DYNAMICS for Sample S1, S2 and S3.

	Monomer (main species)		Aggregates	
	Radius (nm)	Particle concentration (mL^{-1})	Radius (nm)	Particle concentration (mL^{-1})
S1	14.7 ± 0.7	$(8.2 \pm 0.6) \times 10^{13}$	-	-
S2	15.6 ± 0.1	$(2.7 \pm 0.1) \times 10^{13}$	-	-
S3	14.2 ± 0.2	$(6.9 \pm 0.1) \times 10^{13}$	118.2 ± 4.2	$(1.3 \pm 0.1) \times 10^{7}$

Particle concentration

Batch SLS and DLS measurements with the NanoStar and Plate Reader enable rapid quantitation of the particle concentration for both monomodal and multimodal systems. Determining particle concentration requires knowledge of the particle shape—in this case a sphere.

In addition, the refractive index (RI) of the particles and buffer must be specified. DYNAMICS comes pre-loaded with a library of RI values for common materials, and when these are not appropriate, users may specify custom RI values for complex materials like AAVs. RI values of 1.43 and 1.48 were assigned to S1 and S2, respectively,

based on protein and nucleic acid content and empirically validated. With these inputs, the R_h measured by DLS and the static light scattering intensity are used together to provide particle concentration. For typical AAV samples, the concentration measurable by this technique ranges from ~6×10^{10} mL^{-1} to ~1×10^{15} mL^{-1}.

Figure 4 compares the particle concentrations for S1 and S2, obtained with NanoStar and DynaPro Plate Reader, to values determined by the SEC-MALS AAV method described in AN1617. These samples had previously been quantified by SEC-MALS to determine the molar mass, dimer and aggregate content, and the concentration of each species.[4] The SEC-MALS method utilizes a well-validated analysis which is highly accurate and orthogonal to the DLS/SLS method. DYNAMICS reports concentrations of $(8.2 \pm 0.6) \times 10^{13}$ mL^{-1} for S1 and $(2.7 \pm 0.1) \times 10^{13}$ mL^{-1} for S2, respectively. Both NanoStar and DynaPro Plate Reader determined comparable result, within 22% of the SEC-MALS values. This excellent level of agreement means that batch measurements can be used to quickly screen AAVs for capsid concentration.

DYNAMICS can also determine the particle concentrations of multimodal samples, such as sample S3, as shown in Table 2. The monomer concentration of S3 is $(6.9 \pm 0.1) \times 10^{13}$ mL^{-1} and the concentration of larger aggregates was measured as $(1.3 \pm 0.1) \times 10^{7}$ mL^{-1}. Since the degree of DNA loading was unknown, the average RI value of empty and full AAVs was used –1.46.

Three main limitations are encountered for batch concentration measurements by DLS/SLS relative to separation-based techniques such as SEC-MALS or FFF-MALS (FFF is appropriate for particles that are too large for SEC):

1. **Oligomers:** In DLS/SLS the measured R_h value is approximately the z-average of all species present, while the scattered intensity is their weight average. Thus the presence of oligomers leads to underestimation of the concentration. In most cases the accuracy is much better than an order of magnitude.
2. **Size limit:** the upper limit of R_h for concentration measurement is 165 nm for DynaPro Plate Reader and 175 nm for DynaPro NanoStar. This range covers AAVs and just about all viral and non-viral vectors.
3. **RI dependence:** The choice of refractive index significantly impacts the calculation. RI values of 1.43 and 1.48 have been confirmed empirically for empty and full AAVs, respectively, and agree with more rigorous characterization by SEC-MALS.[4] Where the DNA loading is unknown, an average RI of 1.46 may be applied, consistent with literature.[5] However, if 1.46 is selected for the analysis, while the AAVs are in actuality all full and the true RI is 1.48, this error of 1.5% in refractive index leads to an error of 33% in concentration. For screening purposes this discrepancy is usually considered acceptable. Notably, the effect on absolute accuracy does not impact linearity of the analysis for samples with identical composition.

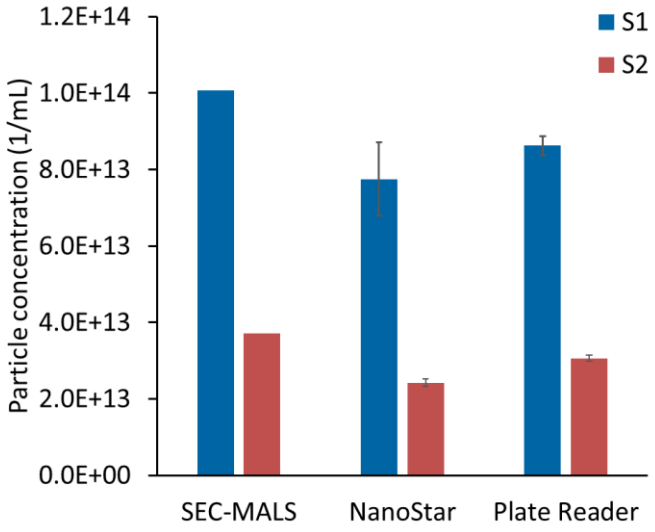

Figure 4. Comparison of viral particle concentration determined in DYNAMICS with those determined by ASTRA's AAV method.

Conclusions

The DynaPro NanoStar and DynaPro Plate Reader offer rapid, low-volume screening of AAV quality attributes via batch static and dynamic light scattering. Both instruments characterize particle size and size distribution, thermal and colloidal stability, and total capsid concentration. These methods are non-destructive and require no method development, making them ideal for incorporation into multiple areas of AAV drug development, process development and quality control.

Acknowledgements

We thank Virovek Inc. for kindly supplying the AAV samples used in this study.

References

1. Hastie, E. & Samulski, R. J. Adeno-Associated Virus at 50: A Golden Anniversary of Discovery, Research, and Gene Therapy Success—A Personal Perspective. *Hum. Gene Ther.* **26**, 257–265 (2015).
2. Naso, M. F., Tomkowicz, B., Perry, W. L. & Strohl, W. R. Adeno-Associated Virus (AAV) as a Vector for Gene Therapy. *BioDrugs* **31**, 317–334 (2017).
3. Wright, J. F. Manufacturing and characterizing AAV-based vectors for use in clinical studies. *Gene Ther.* **15**, 840–848 (2008).
4. Chen, M. & Purchel, A. Quantifying quality attributes of AAV gene therapy vectors by SEC-UV-MALS-dRI. (2019). Available at: https://www.wyatt.com/library/application-notes/an1617-aav-critical-quality-attribute-analysis-by-sec-mals.html
5. Steppert, P. *et al.* Quantification and characterization of virus-like particles by size-exclusion chromatography and nanoparticle tracking analysis. *J. Chromatogr. A* **1487**, 89–99 (2017).